Mode-Switching of the Self-Motion of a Camphor Boat Depending on the Diffusion Distance of Camphor Molecules

Nobuhiko J. Suematsu,[†,‡] Yumihiko Ikura,[§] Masaharu Nagayama,[∥,⊥] Hiroyuki Kitahata,[⊥,#] Nao Kawagishi,[▽] Mai Murakami,[†] and Satoshi Nakata*[,†]

Graduate School of Science, Hiroshima University, Kagamiyama 1-3-1, Higashi-Hiroshima 739-8526, Japan, Meiji Institute for Advanced Study of Mathematical Sciences (MIMS), 1-1-1 Higashimita, Tamaku, Kawasaki 214-8571, Japan, Graduate School of Natural Science and Technology, Kanazawa University, Kakuma-machi, Kanazawa 920-1192, Japan, Institute of Science and Engineering, Kanazawa University, Kakuma-machi, Kanazawa 920-1192, Japan, PRESTO, Japan Science and Technology Agency, 4-1-8, Honcho Kawaguchi, Saitama 332-0012, Japan, Department of Physics, Graduate School of Science, Chiba University, 1-33 Yayoi-cho, Inage-ku, Chiba 263-8522, Japan, and Department of Chemistry, Nara University of Education, Takabatake-cho, Nara 630-8528, Japan

Received: March 1, 2010; Revised Manuscript Received: April 20, 2010

We demonstrated mode-switching of self-motion coupled with diffusion of molecules at a solid/liquid interface. A camphor boat moved spontaneously on water and the mode of self-motion depended on the setup of the boat. When a camphor disk was connected to the center of a larger plastic plate, intermittent motion (alternating between rest and rapid motion) was observed. When the position of the camphor disk was changed from the center to one of its edges, the period of intermittent motion decreased, and intermittent motion changed to continuous motion. The features of this self-motion and mode-switching were qualitatively reproduced by a numerical calculation using a mathematical model that incorporates the distribution of camphor molecules at the solid/liquid interface.

1. Introduction

Self-motion in artificial systems has been investigated to understand a motion in biological systems and to create novel artificial motors that are sensitive to the environment.[1] Several artificial systems that exhibit self-motion have been studied experimentally[2−23] and theoretically[24−27] under almost isothermal and chemical-nonequilibrium conditions. Furthermore, mode-change of self-motion can be demonstrated depending on both the internal conditions (e.g., scraping morphology and chemical structure of the camphor derivative)[28,29] and external conditions (e.g., temperature, surface tension, the shape of the cell, coupling of chemical reactions),[30−37] and the essential features can be reproduced by a computer simulation.[29−34]

Self-motion coupled with a chemical reaction and diffusion is used to show mode-switching of self-motion.[34,36] For example, a 1,10-phenanthroline disk moves spontaneously on an aqueous solution of divalent metal ion and exhibits two modes of self-motion, that is, continuous motion and intermittent motion, where the disk alternates between rapid motion and rest. These two types of self-motion switch, depending on the concentration of metal ion and the stability constant of complex formation.[36] Similar mode-switching was reported in a system coupled with an acid−base reaction.[34] In this case, mode-switching was induced depending on the reaction order.

However, a reaction may not be necessary for a change in the mode of self-motion. A camphor boat, which consists of a camphor disk connected to a plastic plate, shows both continuous and intermittent motion in individual systems without chemical reactions.[32,33,35] In the camphor boat system, the diffusion of camphor molecules at a solid/water interface is important for determining self-motion. In the previous paper, we reported influence of the material and hydrophobicity of the boat, which was effective on the rate of the diffusion of camphor molecules at a solid/liquid interface.[35]

In this study, we focused on the diffusion distance of camphor molecules and its influence on the mode of self-motion and on the period of intermittent motion in a camphor boat system. Both the experimental and numerical results indicated that the features of self-motion depend on the diffusion distance of camphor molecules.

2. Experimental Section

Camphor was obtained from Wako Chemicals (Kyoto, Japan). Water was first filtered through active carbon and an ion-exchange resin and then distilled. A camphor disk (diameter, 3 mm; thickness, 1 mm) was prepared using a pellet die set for FTIR. A camphor boat was prepared by connecting a camphor disk to a polyester plastic plate (thickness, 0.1 mm). The opposing edges of a rectangular plate (width, 8 mm) were bent toward the camphor-attached face at 2 mm (Figure 1), and as a result, the width of the plastic boat was 4 mm. The error in the shape and size of the plastic boat and the attached position of a camphor disk was able to be less than 0.1 mm by printing its design onto the plastic film using PC. It has to be noted that the printed face was not contact with a water surface. The length of the boat (L) and the position at which the camphor disk was attached (p), that is, the distance between the centers of the

* To whom correspondence should be addressed. Tel./Fax: +81-82-424-7409. E-mail: nakatas@hiroshima-u.ac.jp.
[†] Hiroshima University.
[‡] MIMS.
[§] Graduate School of Natural Science and Technology, Kanazawa University.
[∥] Institute of Science and Engineering, Kanazawa University.
[⊥] PRESTO.
[#] Chiba University.
[▽] Nara University of Education.

10.1021/jp101838h
Published on Web 05/11/2010

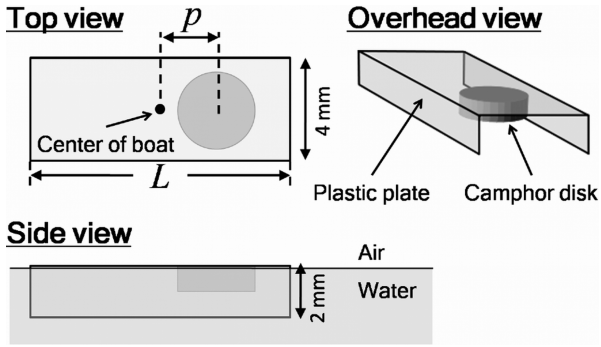

Figure 1. Illustration of the camphor boat. The length L, width, and height of the boat were 3.0−15.0, and 2 mm, respectively. The camphor disk was connected to the plastic plate. The distance between the centers of the boat and the camphor disk was set as p (0.0−4.5 mm).

plastic plate and the camphor disk, were varied (L, 3.0−15.0 mm; p, 0.0−4.5 mm).

The camphor boat was floated on a water surface at room temperature (22 ± 1 °C). A glass Petri dish (diameter, 155 mm; water level, 5 mm) or a rectangle plastic container (width, 200 mm; length, 270 mm; water level, 5 mm) were used to contain the water phase. These containers were large enough to neglect the effect of the boundary. The movement of the camphor boat was monitored with a digital video camera (SONY DCR-VX700, maximum frame rate: 30 fps) and then analyzed on a PC using an image-analysis system "ImageJ 1.41" (National Institutes of Health, U.S.A.). Three or four examinations (with about 6−15 intermittent motions observed for each examination) were performed for the individual experimental conditions; that is, 20−50 data points were used to analyze the features of motion for individual conditions.

Camphor molecules on water were indirectly observed using $CaSO_4$ powder for visualization. Before placement of the camphor boat (L, 9.0 mm; p, 0.0 mm), the powder was spread over the water surface. Then, the boat was floated on water, and the distribution of the powder was monitored by the video camera.

3. Results

The self-motion of the camphor boat showed two characteristic motions: continuous motion and intermittent motion. The former is that the camphor boat moved with a uniform velocity (Figure 2a,b-i). In the latter, the boat repeatedly alternated between rest and rapid motion (Figure 2a,b-ii). After the resting state in intermittent motion (1−5 in Figure 2a,b-ii), the boat suddenly accelerated and moved rapidly (5 and 6 in Figure 2a,b-ii). The boat then slowed (6−20 in Figure 2a,b-ii) and returned to the resting state. This cycle was repeated several times (Figure 2b-ii′).

The mode of self-motion depended on both the position at which the camphor disk was attached p and the boat length L. Under a condition of constant $L = 10.0$ mm, intermittent and continuous motions were observed at $p < 2.0$ mm and $p > 2.0$ mm, respectively. The average velocities in continuous motion were independent of p, with values of about 50 mm·s^{-1} (Figure 2c). Furthermore, the value of p had less of an effect on both the maximum and minimum velocities in intermittent motion; the maximum velocities were about 130 mm·s^{-1} and the minimum velocities were 0 mm·s^{-1} (Figure 2c). Similar to the dependence of p, the mode of self-motion changed with the value of L under a constant value of $p = 0.0$ mm. For $L \geq 5.0$ mm, intermittent motion was seen; otherwise, continuous motion was observed.

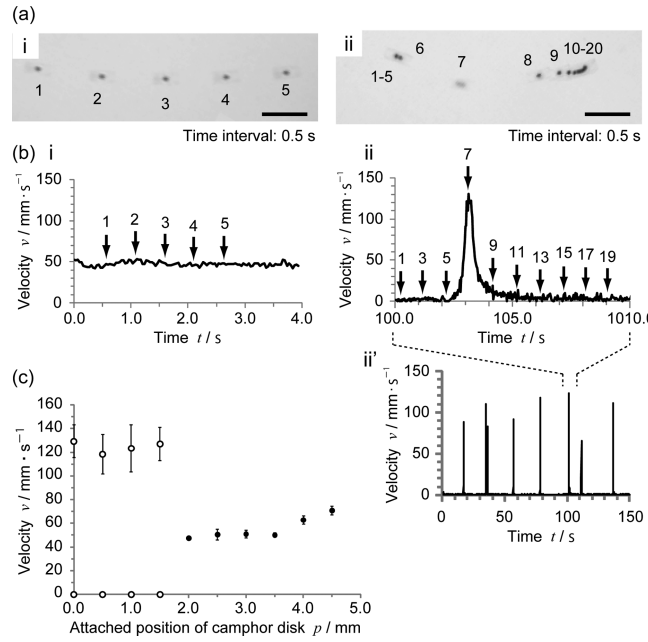

Figure 2. (a) Superimposed photographs (time interval, 0.5 s; scale bar, 20 mm) and (b) time-series of the velocity of self-motion. (i) Continuous motion and (ii) intermittent motion. Black dots in the snapshots indicate the center positions of the boat. The length of the boat L was 10.0 mm, and the distances between the centers of the camphor disk and the plastic plate (p) were (i) 3.0 and (ii) 0.0 mm. (b-ii′) Overview of time-series in intermittent motion. (c) Average velocities in continuous motion (filled circle) and maximum and minimum velocities in intermittent motion (empty circle) depending on the attached position of the camphor disk p. The length of the camphor boat L was 10.0 mm. When $p = 3.5$ mm, the edge of the camphor disk contacts the edge of the boat.

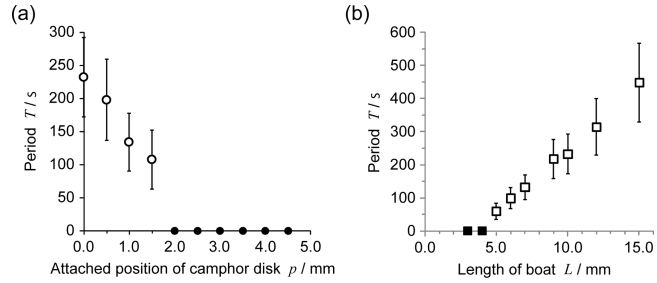

Figure 3. Period of intermittent motion depending on (a) the attached position of the camphor disk p at $L = 10.0$ mm and (b) the length of the camphor boat L at $p = 0.0$ mm. When $p \geq 2.0$ mm or $L \leq 4.0$ mm, continuous motion was observed. The open and filled symbols indicate intermittent motion and continuous motion, respectively.

The period of intermittent motion was also determined by both p and L. First, p was varied for $L = 10.0$ mm. With an increase in p, the period decreased monotonically (Figure 3a) and the self-motion changed to continuous motion at $p \geq 2.0$ mm. Next, L was varied under constant $p = 0.0$ mm. At $L \leq 4.0$ mm, the boat moved with a continuous velocity. The mode changed to intermittent motion at $L \geq 5.0$ mm. The period of intermittent motion increased with an increase in L (Figure 3b).

The symmetry of the boat affected the direction of movement during rapid motion. At $p = 0.0$ mm (symmetrical boat), the direction of movement was random. On the other hand, at $p \neq 0.0$ mm (asymmetrical boat), the boat tended to move toward the edge of the long distance from the camphor disk, and its probability increased with p.

The magnitude of camphor layer roundly developed from its solid was estimated as its radius (see Figure S1 in Supporting Information). Before starting to move, the camphor molecules leaked slowly and the camphor layer slightly spread. Then, the boat accelerated and the camphor layer rapidly expanded. The radius of camphor layer was proportional to the square root of time, which was analogous to typical diffusion process. The rate constant of the development of camphor was $(3.8 \pm 0.2) \times 10^{-3}$ m^2•s^{-1} in the rapid expansion.

4. Discussion

4.1. Mode-Switching of Self-Motion. The self-motion of a camphor boat is driven by the difference in the surface tension around the plastic plate. When camphor molecules develop from one of the open edges, the surface tension decreases and the balance of forces around the plate is broken. As a result, the boat moves in the direction that is opposite to the development of camphor.[32] The camphor molecules dissolve from the camphor disk and diffuse at a solid/liquid interface, and the boat then accelerates when the molecules reach the edge of the plate. Thus, the diffusion process is considered to play an important role in determining the features of self-motion. A rectangular boat has two diffusion distances, that is, the distances between the camphor disk and the edges of the plastic plate. Here, we consider only the shorter distance, because the molecules reach this edge first. The shorter diffusion distance d can be described by p and L as follows:

$$d = \frac{1}{2}L - p - r \tag{1}$$

where r is the radius of the camphor disk ($r = 1.5$ mm).

The stability of uniform-velocity state is shown in Figure 2, while the value of p is varied. To discuss the effect of the diffusion distance d on the stability, the horizontal axis p is transposed to d using eq 1. When the value of d is small enough ($d \leq 1.5$ mm), the boat moves with a uniform velocity ($\sim$50 mm•s^{-1}). For $d > 1.5$ mm, the mode of uniform velocity becomes unstable, and an oscillatory mode generates. Thus, the uniform-velocity state changes to an oscillatory-velocity state with an increase in d.

The period of intermittent motion is considered with reference to the diffusion distance d. In our experiment, the diffusion distance was varied by changing p and L. By changing p, the camphor boat is an asymmetric system where the two diffusion distances are different. In contrast, by changing L, the camphor boat is a symmetrical system, where the camphor disk is attached to the center of the plastic plate ($p = 0.0$). The period of intermittent motion was obtained for both symmetrical (varying L) and asymmetrical (varying p) boats (Figure 3a,b). The period was then replotted against the shorter diffusion distance d (Figure 4). Even though the longer diffusion distances are different between the symmetrical (empty square, filled square) and asymmetrical (empty circle, filled circle) boats, sufficient overlap is observed between two plots. However, mode-switching of self-motion occurred at different diffusion distances; $d = 1.5$ mm for asymmetrical boats and 0.5 mm for symmetrical boats. This difference may be due to the longer diffusion distance and the mass of the boat. The sufficient overlap of the period indicates that the period is determined by d and the longer diffusion distance has less of an effect on the period of intermittent motion.

Here we propose the scenario to explain continuous motion and intermittent motion based on the diffusion of the camphor molecules under the plastic plate. When the diffusion distance d is short enough, camphor molecules dissolved from camphor disk can be constantly supplied to the edge of the boat. As a result, the boat constantly obtains driving force to exhibit continuous motion (Figure 5a). On the other hand, intermittent motion is shown with a large value of d and its period T increases with d. Since the duration of rapid motion is short enough to neglect (ca. 1 s), T is nearly equal to the resting time. During the resting time, camphor molecules diffuse under the plastic plate, reach the edge of the plate, and develop on the water surface (Figure 5b). Thus, the duration of rest might correspond to the diffusion time of camphor molecules at the solid/liquid interface: the relationship between T and d reflects the state of diffusion at the solid/liquid interface.

The value of power index of the relationship between T and d was estimated to be 1.1 based on the experimental results in

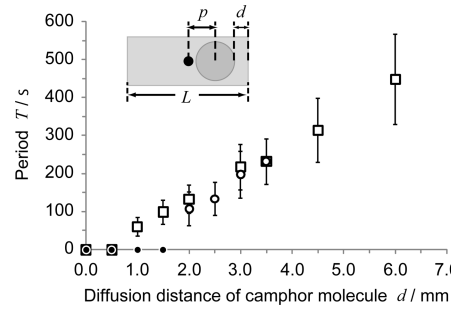

Figure 4. Period of intermittent motion depending on the diffusion distance of camphor molecules (d, see inset). The periods depending on both L and p were plotted on the same graph, when L was changed in the symmetrical system (empty square, filled square) and when p was changed in the asymmetrical system (empty circle, filled circle). The empty and filled symbols indicate intermittent motion and continuous motion, respectively.

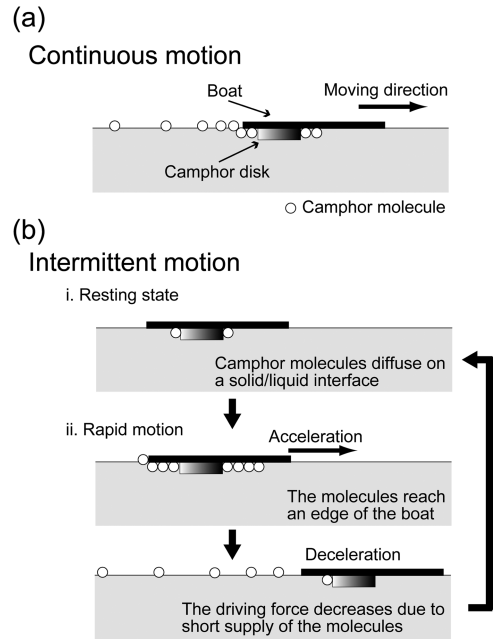

Figure 5. Illustration of the mechanism of self-motion. (a) Continuous motion: The camphor molecules dissolved from camphor disk diffuse to the edge of the boat and are supplied constantly; thus, the driving force is kept constant. (b) Intermittent motion: In the resting state, the molecules dissolve from the camphor disk and diffuse to the edge of the boat. After the molecules reach the edge, the camphor molecules are developed on water, and as a result, the boat accelerated. The molecules accumulated under the plate are spread out on water and disappear. Then, the boat rapidly stops due to the viscous resistance.

Figure 4. Because we assumed that the period corresponds to the diffusion time, this result indicates that the diffusion time is almost proportional to the diffusion distance of camphor molecules at the solid/liquid interface. This result appears to be inconsistent with a general diffusion process where the diffusion time is proportional to the square of the diffusion distance, which means that the power index is 2. However, the power index can be less than 2 under a constant supply of diffusion materials (Appendix 1). Based on the similar discussion, the initial stage of the development of camphor molecules (Figure S1) is considered to be a phenomenon under a constant supply of the molecules from the edge of the boat, because the development is proportional to time. In contrast, the later stage of the development is proportional to the square root of time. Therefore, no camphor molecules might be supplied after moving the boat. However, it has to be noted that the surface development of camphor might be a composite phenomenon including the surface diffusion of molecules and convective flow like the Marangoni flow. Anyhow, even in the slow development at the initial stage, it takes around 1−2 s to develop the length d, which is much shorter than T (∼200 s). Namely, we consider that the development at the air/water interface is faster than the diffusion at the plate/water interface.

4.2. Numerical Calculation for the Mode-Switching of the Self-Motion of a Camphor Boat. Based on our experimental results, we deduce that the intermittent motion originates from the slow diffusion of molecules under the plastic plate. To validate our hypothesis, we introduce a mathematical model for a camphor boat in a one-dimensional system, and qualitatively reproduce the experimental results. The motion of the camphor boat can be expressed by the Newtonian equation:[38,39]

$$m\ddot{x}_p(t) = h(\gamma(u(t,x_f)) - \gamma(u(t,x_b))) - h\mu_0\dot{x}_p(t)(1 + \eta_0|\dot{x}_p(t)|) \quad (2)$$

where m is the mass of the camphor boat, x_p is the center position of the boat, h is the width of the boat, γ is the surface tension depending on u, which is the surface concentration of camphor molecules, x_f and x_b are the positions of the front and back edges of the boat, μ_0 is viscosity, and η_0 is a coefficient. The present model was improved from the previous work (see Supporting Information). The first term in eq 2 represents the difference in surface tension between the front and the back edges of the camphor boat, which acts as a driving force. The surface tension may be expressed as a function of $u(t, x)$ as follows:[30,34]

$$\gamma(u(t,x)) = \begin{cases} \gamma_0, & 0 \le u < u_1 \\ a(u-u_1)+\gamma_0, & u_1 \le u < u_2 \\ b(u-u_2)+\gamma_1, & u_2 \le u < u_3 \\ \gamma_1, & u_3 \le u \end{cases} \quad (3)$$

where γ_0 is the surface tension of pure water, γ_1 is the minimum surface tension depending on the surface concentration of camphor, $a = \gamma_1 - \gamma_0/(u_2 - u_1)(u_3 - u_1)$, $b = \gamma_0 - \gamma_1/(u_3 - u_2)(u_3 - u_1)$, and u_i (i = 1, 2, and 3) are positive constant parameters. The second term in the right-hand side of eq 2 reflects viscose force. The derivation of term $(\eta_0|\dot{x}_p(t)|)$ is described in the Supporting Information.

We next consider a model for the surface concentration of camphor molecules. Based on previous papers,[34,38] we obtain the following reaction−diffusion equation:

$$\frac{\partial u}{\partial t} = \frac{\partial}{\partial x}\left(D(x_p;l_0)\frac{\partial u}{\partial x}\right) - F(x_p,u;l_0) + G(x_c,u;r_0), \quad t>0,\ x \in (0,\Lambda_0) \quad (4)$$

where Λ_0 is the length of the chamber, l_0 is half the length of the boat, and the function D indicates the different diffusion coefficients at the water surface and the plate/water interface, which can be written as follows:

$$D(x_p;l_0) = \begin{cases} D_1, & \left\|x - x_p\right\| \le l_0 \\ D_2, & \left\|x - x_p\right\| > l_0 \end{cases} \quad (5)$$

where we assume that $D_2 \gg D_1$ because the surface diffusion is significantly greater than that at the plate/water interface. The function F represents sublimation, which occurs only at the water surface. Thus, the function can be written as follows:

$$F(x_p,u;l_0) = \begin{cases} 0, & \left\|x - x_p\right\| \le l_0 \\ ku, & \left\|x - x_p\right\| > l_0 \end{cases} \quad (6)$$

where k is the rate of sublimation. The function G expresses the dissolution of camphor molecules from the camphor disk:

$$G(x_c,u;r_0) = \begin{cases} S_0(u_0 - u), & \left\|x - x_c\right\| \le r_0 \\ 0, & \left\|x - x_c\right\| > r_0 \end{cases} \quad (7)$$

where S_0 is the rate constant of dissolution from the camphor disk, u_0 is the saturated concentration of the camphor layer, x_c is the center position of the camphor disk, and r_0 is the radius of the camphor disk. The shorter diffusion distance is defined as $d_0 = l_0 - x_p + x_c - r_0$.

We take the following nonflux boundary conditions

$$\frac{\partial}{\partial x}u(t,0) = \frac{\partial}{\partial x}u(t,l_0) = 0 \quad (8)$$

and initial conditions

$$\begin{cases} u(0,x) \equiv 0 \\ x_c(0) = x_A,\ \dot{x}_c(0) = x_B \end{cases} \quad (9)$$

where x_A and x_B are the initial position and initial velocity of the camphor boat, respectively.

Normalized equations are derived from the above equations. Here we introduce the following dimensionless parameters and variables: $\tau = D_2t/r_0^2$, $y = x/r_0$, $z_c = x_c/r_0$, $\delta = d_0/r_0$, $y_i = x_i/r_0$ (i = p, f, b, A, and B), $\upsilon = u/u_0$, $\Lambda = \Lambda_0/r_0$, $l = l_0/r_0$, $\mu = \mu_0hr_0^2/(mD_2)$, and $\eta = \eta_0D_2/r_0$. The normalized Newtonian equation is

$$\begin{cases} \dfrac{\partial v}{\partial \tau} = \dfrac{\partial}{\partial y}\left(d(y_p;l)\dfrac{\partial v}{\partial y}\right) - f(y_p, v;l) + g(z_c, v) \\ \dot{y}_p = \Gamma(v(\tau, y_f)) - \Gamma(v(\tau, y_b)) - \mu\dot{y}_p(1 + \eta|\dot{y}_p|) \end{cases} \quad \tau > 0,\ y \in (0, \Lambda) \tag{10}$$

The other functions are shown in Appendix 2.

Eq 10 was calculated with varying the diffusion distance δ. The differential equation of v in eq 10 was solved by a semi-implicit scheme, where the spatial variable y was discretized using the finite volume method and the time variable t by the Euler scheme. The Newtonian equation in eq 10 was solved by the Euler scheme with the discretization as described above. The discretization parameters Δt and Δy were 0.01 and 0.2, respectively. A time-series of the velocity of a camphor boat can be obtained from a computer simulation depending on the distance δ (Figure 6). When δ is small enough, the camphor boat moves with a uniform velocity (continuous motion corresponding to Figure 2a,b−i). With an increase in δ, the mode of self-motion changes to intermittent motion (Figure 7). The period of intermittent motion (T_0) decreases and is a power function of δ (Figure 8). The value of the power index in the numerical calculation ($T_0 \propto \delta^{1.23}$) is similar to the experimental value ($T \propto d^{1.1}$). Therefore, this numerical calculation reproduces the experimental results qualitatively.

The mechanism of intermittent motion can be understood using eqs 2−7. In the resting state, the concentration of the camphor molecules u at both edges of the boat is low because of the small diffusion coefficient D_1. Thus, the first term on the right-hand side of eq 2 becomes 0, so the camphor boat cannot obtain the driving force. The camphor molecules gradually accumulate around the camphor disk with an increase in G, as shown by eq 7. The accumulated molecules diffuse and reach the edge of the boat. As a result, the driving force becomes large enough to accelerate the boat.

Furthermore, mathematical model and numerical calculation suggest the conditions that are necessary for intermittent motion. We consider two normalized parameters, that is, $\Delta = D_1/D_2$ and $s = S_0 r_0^2/D_2$. When both parameters are small enough, intermittent motion is seen. A small value of Δ means that the molecular diffusion at the solid/liquid interface is slower than that at the water surface. Similarly, a small value of s indicates that there is only a short supply of camphor molecules to the edge of the boat. Therefore, intermittent motion requires a short supply of camphor molecules to the edge of the boat.

The experimental results and the necessary condition for intermittent motion suggest a scenario for the mode-switching of self-motion. In continuous motion, the boat can constantly develop camphor molecules because of the short diffusion distance to supply molecules to the edge (Figure 5a). On the other hand, in intermittent motion the boat cannot continue moving because of the long diffusion distance, which results in a short supply of camphor molecules to the edge. During the resting time in intermittent motion, camphor molecules do not develop on water but rather diffuse at the solid/liquid interface (Figure 5b). After camphor molecules reach the edge of the plastic plate and spread out on water, the boat accelerates again. This scenario reveals that the mode of self-motion depends on the diffusion distance d.

The influence of convection, for example, Marangoni convection, has to be considered to have an accurate understanding of our experimental results. The convection concurrent with self-motion of a camphor disk has already been reported.[40−42] However, as a first step, we focused on the mode-switching of self-motion depending on the diffusion distance d, and on the mechanism of intermittent motion in this paper.

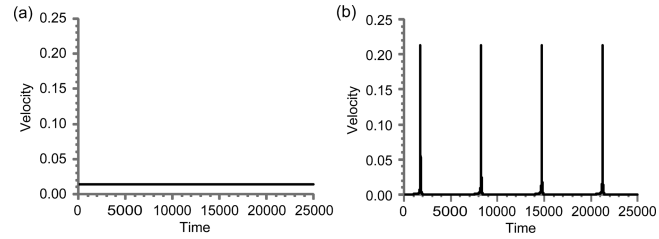

Figure 6. Time variation of velocity of the camphor boat. (a) $\delta = 1.0$ and (b) $\delta = 3.0$. The fixed parameters in (a) and (b) are $L = 500$, $d_1 = 0.0001$, $S = 0.0002$, $\mu = 0.02$, $\Gamma_1 = 1.0$, $\Gamma_0 = 0.1$, $k = 0.01$, $l = 5.0$, $\eta = 50$, $y_A = 20$, $y_B = 0$, $v_1 = 0.001$, $v_2 = 0.2005$, and $v_3 = 0.4$.

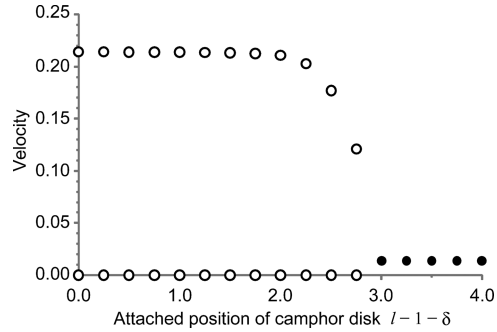

Figure 7. Velocities of self-motion depending on the position at which the camphor disk is attached $l-1-\delta$. Maximum and minimum velocities of intermittent motion (empty circle) and average velocities of continuous motion (filled circle) are plotted.

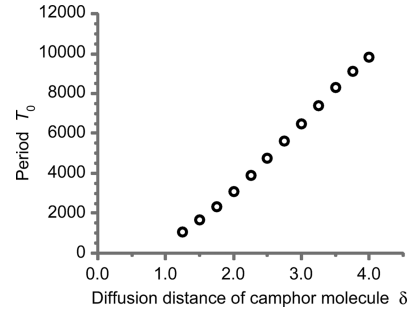

Figure 8. Period of intermittent motion depending on δ. When $\delta <$ 1.0, only uniform motion was observed.

5. Conclusion

The camphor boat showed two types of self-motion, that is, continuous and intermittent motion. With a decrease in the diffusion distance of camphor molecules d, the period of intermittent motion T decreased. The power low between T and d was obtained, and the power index was 1.1 and 1.23 in the experimental and numerical results, respectively. The relationship between T and d originates from the diffusion of camphor molecules under the plastic plate with a constant supply of camphor molecules. When d is smaller than the critical value d_c (1.5 mm for an asymmetrical boat and 0.5 mm for a symmetrical boat), self-motion switches to continuous motion. These results were reproduced with a mathematical model, which suggested that intermittent motion required the short supply to the edge of the camphor boat. In conclusion, we proposed novel mechanism to control mode of self-motion.

Acknowledgment. The present study was supported in part by a Grant-in-Aid for Scientific Research C (No. 21340023) and a grant from the Asahi Glass Foundation to S.N., a Grant-in-Aid for Scientific Research B (No. 20550124) to M.N., a

Grant-in-Aid for Scientific Research for Young Scientists B (No.21740282) to H.K., and a Grant-in-Aid for the Global COE Program "Formation and Development of Mathematical Sciences Based on Modeling and Analysis".

APPENDIX 1: POWER LAW FOR DIFFUSION UNDER A CONSTANT SUPPLY

The relationship between the period of intermittent motion, T, and the shorter diffusion distance, d, as shown in Figure 4 (experiment) and Figure 8 (numerical calculation) can be discussed by considering diffusion with a constant supply. This process in a one-dimensional system can be described as follows:

$$\frac{\partial u}{\partial t} = D\frac{\partial^2 u}{\partial x^2} + k\delta(x) \tag{A1}$$

where D is the diffusion constant and k is the rate of supply. The solution for eq A1 with an initial condition of $u(x) = 0$ can be written using the Green function method:

$$u(x,t) = k\sqrt{\frac{t}{\pi D}}\exp\left(-\frac{x^2}{4Dt}\right) - \frac{kx}{2D}\left(\mathrm{sgn}(x) - \mathrm{erf}\left(\frac{x}{\sqrt{4Dt}}\right)\right) \tag{A2}$$

where $\mathrm{sgn}(x)$ is a step function defined as

$$\mathrm{sgn}(x) = \begin{cases} 1 & (x > 0) \\ 0 & (x = 0) \\ -1 & (x < 0) \end{cases}$$

and $\mathrm{erf}(x)$ is an error function defined as

$$\mathrm{erf}(x) = \frac{2}{\sqrt{\pi}}\int_0^x \exp(-x'^2)\mathrm{d}x'$$

Using eq A2, we can calculate the change with time in the position x at which u has a constant value

$$\frac{\partial x}{\partial t} = -\left(\frac{\partial u}{\partial t}\right)/\left(\frac{\partial u}{\partial x}\right) = \sqrt{\frac{D}{\pi t}}\frac{\exp(-x^2/4Dt)}{1 - \mathrm{erf}(x/\sqrt{4Dt})} \tag{A3}$$

for $x > 0$.

If x and t obey the power law, $t \propto x^n$, n can be written as

$$\frac{1}{n} = \frac{\partial(\ln x)}{\partial(\ln t)} = \frac{t}{x}\frac{\partial x}{\partial t} = \sqrt{\frac{Dt}{\pi x^2}}\frac{\exp(-x^2/4Dt)}{1 - \mathrm{erf}(x/\sqrt{4Dt})} = \frac{1}{\sqrt{4\pi}}\frac{\exp(-s^2)}{s(1 - \mathrm{erf}(s))} \tag{A4}$$

where $s = x/(4Dt)^{1/2}$. According to de l'Hopital's theorem

$$\lim_{s\to\infty}\frac{1}{n} = \lim_{s\to\infty}\frac{1}{\sqrt{4\pi}}\left[\frac{\exp(-s^2)/s}{1 - \mathrm{erf}(s)}\right] = \lim_{s\to\infty}\frac{1}{\sqrt{4\pi}}\frac{(2s^2 + 1)\exp(-s^2)}{\sqrt{4/\pi}s^2\exp(-s^2)} = \frac{1}{2}$$

We can also show

$$\frac{1}{\sqrt{4\pi}}\frac{\exp(-s^2)/s}{1 - \mathrm{erf}(s)} - \frac{1}{2} = \frac{1}{\sqrt{4\pi}}\frac{\exp(-s^2)/s - (1 - \mathrm{erf}(s))\sqrt{\pi}}{1 - \mathrm{erf}(s)} > \frac{1}{2}$$

for $s > 0$ by setting

$$f(s) = \frac{\exp(-s^2)}{s} - \sqrt{\pi}(1 - \mathrm{erf}(s)) = \frac{\exp(-s^2)}{s} - 2\int_s^\infty \exp(-s'^2)\mathrm{d}s'$$

and showing that

$$\lim_{s\to\infty} f(s) = \frac{1}{\sqrt{4\pi}}\left[\frac{\exp(-s^2)}{s} - 2\int_s^\infty \exp(-s'^2)\mathrm{d}s'\right] = 0$$

and

$$\frac{\mathrm{d}}{\mathrm{d}s}f(s) = -\frac{(2s^2 + 1)\exp(-s^2)}{s^2} + 2\exp(-s^2) = -\frac{\exp(-s^2)}{s^2} < 0$$

Therefore, the power index, n, is

$$0 < n < 2 \tag{A5}$$

which corresponds to both experimental and numerical results.

APPENDIX 2: NORMALIZATION OF THE MATHEMATICAL MODEL

Here, we show the results of the normalization of eqs 2−9. Let us introduce the following dimensionless parameters and variables, that is, $\tau = D_2 t/r_0^2$, $y = x/r_0$, $z_c = x_c/r_0$, $\delta = d_0/r_0$, $y_i = x_i/r_0$ (i = p, f, b, A, and B), $v = u/u_0$, $\Lambda = \Lambda_0/r_0$, $l = l_0/r_0$, $\mu = \mu_0 h r_0^2/(mD_2)$, and $\eta = \eta_0 D_2/r_0$. We derive the following dimensionless model equation:

$$\begin{cases} \dfrac{\partial v}{\partial \tau} = \dfrac{\partial}{\partial y}\left(d(y_p;l)\dfrac{\partial v}{\partial y}\right) - f(y_p, v; l) + g(z_c, v) \\ \ddot{y}_p = \Gamma(v(\tau, y_f)) - \Gamma(v(\tau, y_b)) - \mu\dot{y}_p(1 + \eta|\dot{y}_p|) \end{cases} \tau > 0,\ y \in (0, \Lambda) \tag{A6}$$

with initial conditions

$$\begin{cases} v(0, y) \equiv 0 \\ y_p(0) = y_A,\ \dot{y}_p(0) = y_B, \end{cases} \tag{A7}$$

and boundary conditions

$$\frac{\partial}{\partial y}v(\tau, 0) = \frac{\partial}{\partial y}v(\tau, \Lambda) = 0 \tag{A8}$$

where $\Gamma(v)$, $\Delta(y_p; l)$, $f(y_p, v; l)$, and $g(z_c, v)$ are expressed as follows:

$$\Gamma(v) = \begin{cases} \Gamma_0, & 0 \le v \le v_1 \\ A(v - v_1)^2 + \Gamma_0, & v_1 < v \le v_2 \\ B(v - v_3)^2 + \Gamma_1, & v_2 < v \le v_3 \\ \Gamma_1, & v > v_3 \end{cases} \quad \text{(A9)}$$

$$d(y_p;l) = \begin{cases} \Delta, & ||y_p - y|| \le l \\ 1, & ||y_p - y|| > l \end{cases} \quad \text{(A10)}$$

$$f(y_p, v;l) = \begin{cases} 0, & ||y_p - y|| \le l \\ kv, & ||y_p - y|| > l \end{cases} \quad \text{(A11)}$$

and

$$g(z_c, v) = \begin{cases} S(1 - v), & ||z_c - y|| \le 1 \\ 0, & ||z_c - y|| > 1 \end{cases} \quad \text{(A12)}$$

If we use dimensionless parameters, $\Gamma_i = hr_0^3\gamma_i/(mD_2^2)$ (i = 0 or 1), $v_i = u_i/u_0$ (i = 1, 2, or 3), $A = (\Gamma_1 - \Gamma_0)/\{(v_3 - v_2)(v_2 - v_1)\}$, $B = (\Gamma_0 - \Gamma_1)/\{(v_3 - v_2)(v_3 - v_1)\}$, $\Delta = D_1/D_2$, $k = r_0^2k_0/D_2$, and $S = r_0^2S_0/D_2$.

Supporting Information Available: Additional figures and derivations. This material is available free of charge via the Internet at http://pubs.acs.org.

References and Notes

(1) Mikhailov, A.; Meinköhn, D. *Self-Motion in Physico-Chemical Systems Far From Thermal Equilibrium*; Springer: Berlin, Heidelberg, 1997; Vol. 484.
(2) Yoshida, R.; Sakai, T.; Ito, S.; Yamaguchi, T. *J. Am. Chem. Soc.* **2002**, *124*, 8095–8099.
(3) Lorenceau, É.; Quéré, D. *J. Fluid Mech.* **2004**, *510*, 29–45.
(4) Yamaguchi, T.; Shinbo, T. *Chem. Lett.* **1989**, 935–936.
(5) Ichimura, K.; Oh, S.-K.; Nakagawa, M. *Science* **2000**, *288*, 1624–1626.
(6) Chaudhury, M. K.; Whitsides, G. M. *Science* **1992**, *256*, 1539–1541.
(7) Brochard, F. *Langmuir* **1989**, *5*, 432–438.
(8) Ichino, T.; Asahi, T.; Kitahata, H.; Magome, N.; Agladze, K.; Yoshikawa, K. *J. Phys. Chem. C* **2008**, *112*, 3032–3035.
(9) Stoilov, Y. Y. *Langmuir* **1998**, *14*, 5685–5690.
(10) Bain, C. D.; Burnett-Hall, G.; Montgomerie, R. *Nature* **1994**, *372*, 414–415.
(11) dos Santos, F. D.; Ondarçuhu, T. *Phys. Rev. Lett.* **1995**, *75*, 2972–2975.
(12) Nakata, S.; Komoto, H.; Hayashi, K.; Menzinger, M. *J. Phys. Chem. B* **2000**, *104*, 3589–3593.
(13) Paxton, W. F.; Sundarajan, S.; Mallouk, T. E.; Sen, A. *Angew. Chem., Int. Ed.* **2006**, *45*, 5420–5429.
(14) Sumino, Y.; Magome, N.; Hamada, T.; Yoshikawa, K. *Phys. Rev. Lett.* **2005**, *94*, 068301.
(15) Sumino, Y.; Yoshikawa, K. *Chaos* **2008**, *18*, 026106.
(16) Hong, Y.; Velegol, D.; Chaturvedi, N.; Sen, A. *Phys. Chem. Chem. Phys.* **2010**, *12*, 1423–1435.
(17) Chang, S. T.; Paunov, V. N.; Petsev, D. N.; Velev, O. D. *Nat. Mater.* **2007**, *6*, 235–240.
(18) Schulz, O.; Markus, M. *J. Phys. Chem. B* **2007**, *111*, 8175–8178.
(19) Su, M. *Appl. Phys. Lett.* **2007**, *90*, 144102.
(20) Quéré, D.; Ajdari, A. *Nat. Mater.* **2006**, *5*, 429–430.
(21) Nagai, K.; Sumino, Y.; Kitahata, H.; Yoshikawa, K. *Phys. Rev. E* **2005**, *71*, 065301.
(22) Soh, S.; Bishop, J. M. K.; Grzybowski, B. A. *J. Phys. Chem. B* **2008**, *112*, 10848–10853.
(23) Luo, C.; Qiao, L.; Li, H. *Microfluid. Nanofluid.* **2010**, DOI: 10.1007/s10404-010-0569-4.
(24) de Gennes, P. G. *Phys. A* **1998**, *249*, 196–205.
(25) Jülicher, F.; Ajdari, A.; Prost, J. *Rev. Mod. Phys.* **1997**, *69*, 1269–1281.
(26) Astumian, R. D.; Bier, M. *Phys. Rev. Lett.* **1994**, *72*, 1766–1769.
(27) Sekimoto, K. *Prog. Theor. Phys.* **1998**, *130*, 17–27.
(28) Nakata, S.; Kirisaka, J.; Arima, Y.; Ishii, T. *J. Phys. Chem. B* **2006**, *110*, 21131–21134.
(29) Nakata, S.; Iguchi, Y.; Ose, S.; Kuboyama, M.; Ishii, T.; Yoshikawa, K. *Langmuir* **1997**, *13*, 4454–4458.
(30) Hayashima, Y.; Nagayama, M.; Nakata, S. *J. Phys. Chem. B* **2001**, *105*, 5353–5357.
(31) Kohira, M. I.; Hayashima, Y.; Nagayama, M.; Nakata, S. *Langmuir* **2001**, *17*, 7124–7129.
(32) Nakata, S.; Hiromatsu, S. *Colloids Surf., A* **2003**, *224*, 157–163.
(33) Nakata, S.; Matsuo, K. *Langmuir* **2005**, *21*, 982–984.
(34) Nagayama, M.; Yadome, M.; Murakami, M.; Kato, N.; Kirisaka, J.; Nakata, S. *Phys. Chem. Chem. Phys.* **2009**, *11*, 1085–1090.
(35) Nakata, S.; Kawagishi, N.; Murakami, M.; Suematsu, N. J.; Nakamura, M. *Colloids Surf., A* **2009**, *349*, 74–77.
(36) Nakata, S.; Arima, Y. *Colloids Surf., A* **2008**, *324*, 222–227.
(37) Bassik, N.; Abebe, B. T.; Gracias, D. H. *Langmuir* **2008**, *24*, 12158–12163.
(38) Hayashima, Y.; Nakagayama, M.; Doi, Y.; Nakata, S.; Kimura, M.; Iida, M. *Phys. Chem. Chem. Phys.* **2002**, *4*, 1386–1392.
(39) Nagayama, M.; Nakata, S.; Doi, Y.; Hayashima, Y. *Phys. D* **2004**, *194*, 151–165.
(40) Kitahata, H.; Hiromatus, S.; Doi, Y.; Nakata, S.; Islam, M. R. *Phys. Chem. Chem. Phys.* **2004**, *6*, 2409–2414.
(41) Kovalchuk, V. I.; Kamusewitz, H.; Vollhardt, D.; Kovalchuk, N. M. *Phys. Rev. E* **1999**, *60*, 2029–2036.
(42) Kovalchuk, N. M.; Kovalchuk, V. I.; Vollhardt, D. *Phys. Rev. E* **2001**, *63*, 031604.

JP101838H